

Research Article

# Science and Technology in Biomedical Engineering: Labacs Case Example

**Cecic M<sup>1</sup>, Papic V<sup>1</sup>, Bonkovic M<sup>1</sup>, Grujic T<sup>1\*</sup>, Music J<sup>1</sup>, Kuzmanic-Skelin A<sup>1</sup>, Stancic I<sup>1</sup>, Marasovic T<sup>1</sup>, Cic M<sup>1</sup> and Plestina V<sup>2</sup>**

<sup>1</sup>Laboratory of Biomechanics, University of Split, Croatia

<sup>2</sup>Faculty of Science, University of Split, Croatia

**\*Corresponding author:** Grujic T, Laboratory of Biomechanics and Automatic Control Systems – LaBACS, Faculty of Electrical Engineering, Mechanical Engineering and Naval Architecture, University of Split, R. Boskovicica 32, 21000 Split, Croatia

**Received:** July 31, 2014; **Accepted:** September 05, 2014; **Published:** September 09, 2014

## Abstract

This paper presents the scientific efforts of the group of engineers and scientists from the Laboratory of Biomechanics and Automatic Control Systems – LaBACS, Faculty of Electrical Engineering, Mechanical Engineering and Naval Architecture, University of Split, Croatia. The field of our expertise is biomedical engineering, and we are dedicated to finding the solutions for various current biomedical engineering problems. The primary goal of our research interests is to develop new, state-of-the-art, cost-effective biomedical and biomechanical measurement systems and to apply them on the human subjects to obtain scientifically significant results. This paper presents a short review of some of our newly developed measurement systems and digital signal processing techniques and algorithms for processing and analysis of the measured biomechanical and biomedical signals.

**Keywords:** Biomechanics of human movements; 3D Optical motion tracking system; Inertial sensors; Computer vision; Biosignals; Human anthropometric parameters

## Introduction

Biomedical engineering or bioengineering can be defined as the application of engineering techniques to the understanding of biological systems of the human, and to the development of therapeutic techniques, bioinstrumentation, and biosensors, among other. Bioengineering is relatively new, but multidisciplinary research field which combines knowledge and principles from electrical and mechanical engineering, computer science, biology, medicine, chemistry, etc. Therefore, biomedical engineering as a scientific discipline can be divided into a whole range of research fields including biomechanics, biosignals, bioinstrumentation, biosensors, biomaterials, biomolecular engineering – let us mention only few of them. The main goal of each of these fields is to improve the quality of human life not only in illness, but in wellness, as well.

At the Laboratory for Biomechanics and Automatic Control Systems - LaBACS, at the Faculty of Electrical Engineering, Mechanical Engineering and Naval Architecture, University of Split, Croatia, a group of electrical and computer science engineers and scientists have specialized different subfields of biomedical engineering research and education. Our research interests include biomechanics of human movements, biosignals measurement, analysis, identification, and classification, and development and application of bioinstrumentation and biosensors.

Biomechanics involves the precise description of human movements and the study of the causes of human movement [1]. The study of biomechanics is relevant to professional practice in many professions related to kinesiology, sport and medicine. For example, the physical educator or coach who is teaching movement technique and the athletic trainer or physical therapist treating an injury uses biomechanics to qualitatively analyze movement [1]. Therefore, the precise measurement and analysis of human movements is an

essential step in biomechanical research used in sports and medicine. It can include various methods and technologies because of large range of possible applications.

Regarding the term of biosignal; it implies a broad spectrum of different signals, from Electroencephalograms (EEG), Electrocardiograms (ECG), and Electromyograms (EMG) which measure the electrical activity of muscles during contraction, to the biomechanical signals such as kinematics data of human motion (motion trajectories, velocities and accelerations). Biosignals measurement, processing, analysis, identification and classification are a wide research area for itself. As an example, biosignal processing involves the use of signal processing techniques for the interpretation of physiological measurements and the understanding of physiological systems [2]. Although the computerized analytical techniques of signal processing are obtained mostly from engineering fields such as telecommunications and applied mathematics, the nature of physiological data requires substantial biological understanding for its interpretation [2].

Design and development of bioinstrumentation and biosensors, including biosignal processing and classification software, require an extensive knowledge and experience in different engineering fields like electrical and mechanical engineering, computer science, artificial intelligence, and machine learning.

The research done by LaBACS in the area of biomedical engineering is recognized through research grants and numerous publications in international scientific journals [3-8]. The intention of this review paper is to shortly present our new achievements in some of the research areas in which we are currently involved. The paper is organized in four major sections, as follows:

In Section 2; our multimodal approaches to the field of biomechanics of human movements are presented. We have

designed, developed, and tested several different systems for human motion tracking and detection which will be described in this paper in the following manner:

The first approach is the design, development, and evaluation of optical motion-tracking system based on active white light markers [3]. The whole system is developed as an affordable (low cost) kinematics measurement system for laboratories where commercial 'gold standard' motion-capturing systems such as Vicon [9] and Optotrak [10] are unavailable. The novelty of our approach really rests with the experimental setup and application of the system to measurement of human kinematics. The use of cost-effective visible light LED markers, and two low-cost fast cameras, instead of expensive Infrared (IR) markers and IR cameras is the novelty itself, as well. The system is intended to be used in measurement of human motions in laboratory conditions (activities like human gait, treadmill walking, and some in-door individual sport activities like cycling and ergo meter rowing).

The second approach aims to overcome the drawbacks of the first one (system implementation only in laboratory conditions and only on individuals). Therefore, we developed the system based on image processing procedures which detects the objects (humans) in demanding backgrounds such as water [11]. We tested our system in case of tracking players in water polo and the obtained results showed the validity and efficiency of our proposed system.

Many biomechanical analyses are interested in the estimation of the pose (position and orientation) of body segments. In particular, head pose estimation is of relevance for both, kinematics data acquisition and head range of motion evaluation. While pose inference can be made with many commercially available optoelectronic systems and inertial measurement units, computer vision techniques draw research attention since they provide a cost-effective solutions to body segment pose estimation. Therefore, as a third approach to human movement, we developed a computer-vision method which estimates head pose from uncalibrated monocular images [12]. Our method is based on a weak perspective projection model of camera and a triangular face model.

Besides three previously mentioned motion-tracking techniques, our fourth approach is oriented toward implementation of inertial Micro-Electro-Mechanical (MEMS) sensors. In the field of human motion tracking, inertial sensors have become attractive alternative to optoelectronic methods since they are usually more cost effective and they have higher mobility and lower subject set-up time [4-13]. As an alternative to computer-vision based human pose detection, previously described, we proposed the system based on inertial sensors. In this case, our system was implemented on a problem of human head pose estimation with the aim of using head motion as a means of controlling computer pointer and different objects (like robot manipulator) by subjects with no control over upper limbs [6].

Apart from the third and fourth approaches, that were oriented toward detection of head pose, our fifth approach is focused on detection and recognition of other body part movements. We developed gesture recognition system which also implements MEMS inertial sensor (three-dimensional accelerometer build into smart phone) [14,15]. Our system uses advanced machine

learning algorithms, specifically, distance metric learning for gesture classification and is capable to recognize nine different gestures performed by a human, with very high accuracy.

Section 3: Deals with biosignal measurement, analysis, identification and classification. In this paper we will present two of our different applications of biosignal processing:

Regarding biosignals, first research interest was focused on gait patterns of human and humanoid robots [7]. Human (or humanoid robot) gait is often described by changes in angular rotation, angular velocity, and angular acceleration of hip, knee and ankle joints during one gait cycle. Using optical measurement system, developed in our laboratory [3], we performed measurement on 30 healthy barefoot humans while walking on a treadmill. We also simulated types of irregular gait, by measurements on subjects wearing knee constraints. By analyzing obtained measurement results, we proposed new kinematics parameters (among which is so-called Gait Factor) which clearly indicate the discrepancy between normal, healthy gait trials and irregular gait trials. We showed that the proposed Gait Factor parameter is a valuable measure for the detection of irregularities in gait patterns of humans and humanoid robots.

The second focus of our biosignal research is dealing with EEG signals. The purpose of our work was to perform the efficient and automatic classification of sleep stage, based on features extracted from measured EEG signals [8]. We analyzed EEG signals of 20 healthy babies, during daytime sleep. We proposed novel feature vectors of a single EEG channel, and performed sleep stage classification by using the Support Vector Machine (SVM) classification algorithm. We obtained high classification accuracy, higher than the human experts' agreement, which confirms our method as an efficient procedure for automatic sleep stage classification.

Section 4: Deals with human anthropometric parameters estimation. Obtaining accurate anthropometric body segment parameters in a fast and reliable manner is an essential step in biomechanical analysis of human motion. With advance of computer vision, and reduction in cost of electronic components, building a customized computer-vision based measurement device becomes possible. Therefore, we developed 3D structured light scanner for anthropometric parameter estimation, consisting of stereovision system with one active sensor (LPD projector) and one passive sensor (camera) [5]. We proposed novel structured light pattern for 3D scanner. The efficacy and accuracy of the proposed system was tested both on artificial objects with known dimensions, and on eight human subjects.

## Human Motion Tracking and Detection

### Optical motion-tracking system based on active white light markers

Our objective was to design, develop, and validate a simple and cost-effective kinematics measurement system with sub-pixel accuracy [3]. The novelty of the developed system is its design, which is based on LED markers operating with visible light, rather than the IR markers or passive reflective markers that are commonly used. The backbone of the developed system is a pair of high-speed industrial cameras. Calibration procedures and a super-resolution

marker model were introduced, ensuring sub-pixel marker centre detection which in final resulted with higher 3D reconstruction accuracy. Evaluation of the system consisted of an accuracy test for stationary and dynamic objects. Major limitations of any marker-based optical tracking systems are marker occlusion by body parts and marker aliasing, and inoperability in dynamic lighting conditions (outdoors). Skin-mounted marker trajectories measured with optical motion capture systems are considered as an adequate representation of the underlying bone trajectories, even though there is an evident motion between the bone and a skin-mounted marker. Despite these drawbacks, optoelectronic devices are today the major tool used for tracking the movements of a human body. Unlike other methods, they offer a complete solution, since they enable simple reconstruction in all three spatial dimensions of the global coordinate system, and are relatively simple to build. Implementation of these systems in laboratories has resulted in a higher quality of research and many clinical applications.

### Materials and Methods

Proposed system was developed as an affordable measurement system for laboratories where commercial systems such as Vicon and Optotrak are unaffordable. Improvement of the accuracy (resolution) of the measurement system was achieved by introduction of an image super-resolution technique, which pre-processes the observed image frames, and determines the location of objects in the analyzed frames. Measurement system (depicted in Figure 1) includes both hardware and software components. The main hardware component is a pair of Basler 602fc high speed digital cameras, capable of feeding the computer at a rate of 100 frames per second with resolution of 560 X 490 pixels. Body markers were manufactured using a 3mm flat-top LEDs with light intensity of 10 Cd. Special plastic housings were used for holding the LEDs and for their optimal placement on a body surface. Software components include procedures for camera distortion removal, system calibration, marker detection, tracking and 3D marker position reconstruction. A user-friendly interface was designed, offering initial marker identification and final representation of the measured and analyzed kinematics data in 3D space.

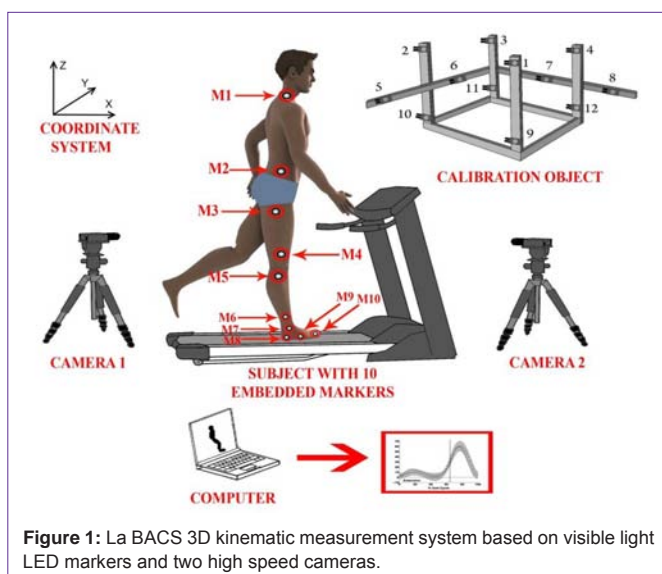


Figure 1: La BACS 3D kinematic measurement system based on visible light LED markers and two high speed cameras.

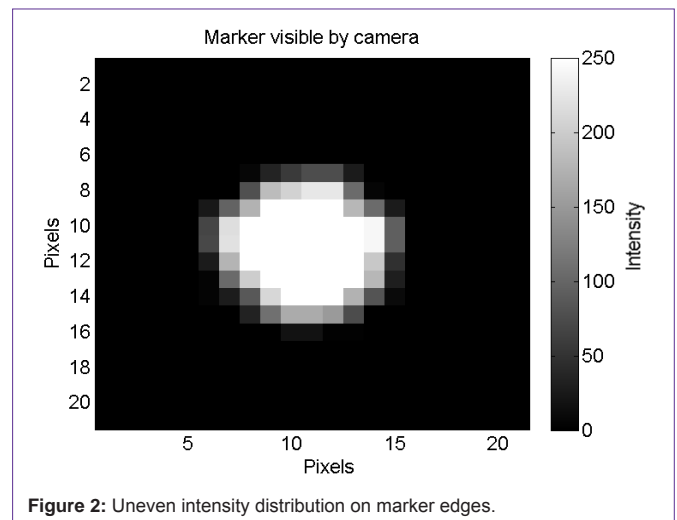


Figure 2: Uneven intensity distribution on marker edges.

### System accuracy improvement

Capturing images of an object in space is a procedure that takes discrete samples of the continuous object’s surface and records them in the memory in a form of image pixels. The introduced super-resolution method utilizes the marker’s intensity distribution on a captured image: in real conditions, when the marker is not perfectly centered with the camera’s pixel centre, marker intensity decreases non-uniformly on its edges. Light emitted from light source is distributed upon camera’s several neighboring pixels, as shown in Figure 2. The intensity slope on the marker edge is following Gaussian curve. This property is utilized in the calculation of an exact marker centre location. The proposed marker model is based on a 2D Gaussian curve, which is presented with equation (1), where  $I$  is intensity at the desired location  $(x,y)$  around the marker centre,  $A$  is maximum intensity, and  $\sigma$  is standard deviation.

$$I(x, y) = Ae^{-(x^2+y^2)/(2\sigma^2)} \tag{1}$$

While having acceptable marker model, it is possible to determine marker center location inside single camera pixel. For the sake of computing time, algorithm is set to calculate marker center in 1/20 of pixel size (while other division are also possible).

### Results

The results of the accuracy trial in static laboratory conditions for 100 markers are presented in Table 1. A comparison of 3d errors in the cases with and without application of the sub-pixel algorithm is shown. The system has a mean absolute 3D error of 0.2009mm with standard deviation of 0.1642mm. Currently, the developed system is widely used for biomechanical research in LaBACS. However, future work is required to perform motion analysis of more complicated movements (where marker occlusion is frequent), by adding more cameras, and to include an algorithm for automatic detection and identification of markers based on a human body model.

### Detection of global movements of multiple persons based on image processing

Systems for tracking team movements in sports are dominantly focused on the most popular games such as football [16] and

**Table 1:** Results of accuracy test in static conditions.

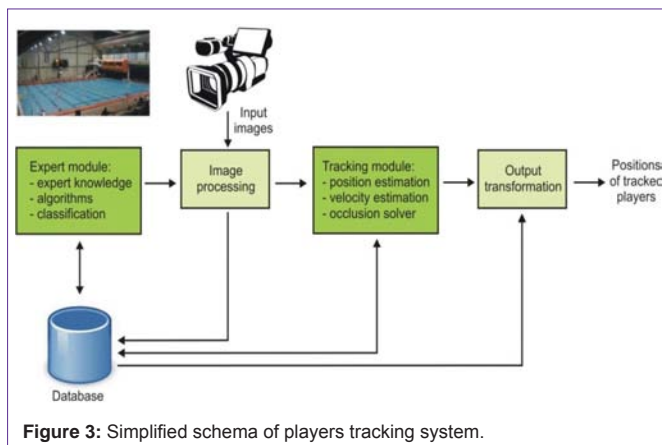
		3D (with sub-pixel algorithm)	3D (without sub-pixel algorithm)
Error [mm]	mean	0.2009	2.8420
	std	0.1642	2.3540
	RMSE	0.2698	4.5815
Error [pix]	mean	0.0490	0.6937
	std	0.0401	0.5746
	RMSE	0.06583	1.11798

basketball [17]. We focused our research on application of tracking players in water polo having in mind that this application has some interesting specificities that should be addressed adequately [11]. General but much simplified system architecture is presented in Figure 3. For category classification we used supervised classification that uses training sets of object images to create descriptors for each defined class. The training sets are selected manually to represent a common picture set of that class. The classifier method then analyzes the training set and generates a descriptor for that particular class. This descriptor could then be used on other object images, which determines if that image is a part of that class.

Particular interest is on development of image processing procedures that can cope well with problem of object detection in scenes with dynamic background such as water. For this purpose, we proposed a novel method for pixel classification. Luminance was separated from YCbCr color space and optimal 2D color plane and 3D color space for pixels set classification defined. 2D color plane classification is based on Euclidean distance while 3D color space classification is based on the use of bivariate histograms. Obtained results showed the validity and efficiency of the proposed approach [11]. It is important to point out that this approach could be used for other applications dealing with tracking objects in water, not only sports related. Therefore, our future work will be oriented in that direction.

**Head pose estimation using computer vision and facial anthropometric parameters**

In LaBACS, a computer-vision method has been developed which estimates head pose from uncalibrated monocular images [5]. The approach addresses the problem of 3D configuration reconstruction of head using 2D spatial information of locations of facial features in images and anthropometric parameters of face.



**Description of computer – vision method for pose estimation**

Proposed method is based on a weak perspective projection model of camera and a triangular face model. According to [18], the 3D object pose estimation from 2D is possible for any rigidly connected structure when following assumptions hold:

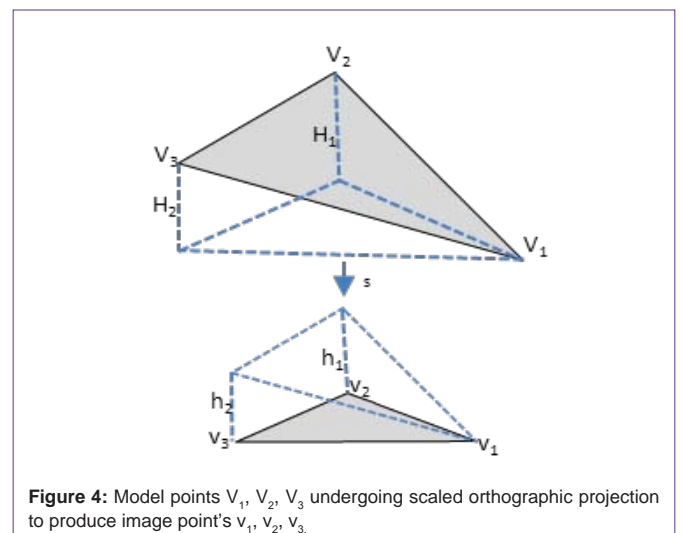
1. The image formation can be closely approximated by a weak-perspective projection model.
2. The image coordinates of the points between connected segments are known.
3. The relative lengths of the segments are known.

In order to apply weak-perspective projection model, local depth of the object of interest must be small compared to the distance between object and camera, which is applicable in many image acquisition setups. Weak-perspective projection is exemplified in Figure 4. And can be described as a scaled orthographic model with equation (2), where  $s$  is the unknown camera scale,  $[X,Y,Z]^T$  are 3D coordinates of model point,  $[x,y]^T$  are corresponding image coordinates.

$$\begin{bmatrix} x \\ y \end{bmatrix} = s \begin{bmatrix} X \\ Y \\ Z \end{bmatrix} \tag{2}$$

The system described with (2) is under-constrained and will consequently produce more than one solution. This is due to unknown scale parameter and inability to resolve relative depth ambiguity. In our method constraints are proposed to remove recovery ambiguity.

Head can be represented as a 3D rigid body within the 3D coordinate system. Geometry for such a head model is obtained from anthropometric measurements of distances between natural landmarks such as eyes, nose, mouth, ears, etc. As the most distinguishing features of the face are eyes and mouth, we represent the head with the simple triangular model defined by three vertices  $V_i(X,Y,Z), i = 1..3$ . These vertices, in image coordinates, correspond



to centers of eyes and the middle point between mouth corners, denoted as  $v_i(x,y)$ . More complex model would include the detection of other facial features, like nose, ears and different face marks which are skin-colored and are hard to detect. The anthropometry from [19] is adopted:  $d(V_1, V_2)=d(V_3, V_2)$  ;  $d(V_1, V_3)=6.45$  cm ;  $d(V_1, V_3)= 1.22 d(V_1, V_2)$ .

The approach to computing the pose of triangular model from three corresponding points in monocular image follows the work of [20]. To recover 3D pose of a model it is required to know the length of segments between vertices ( $D_{12}, D_{23}, D_{13}$ ) and corresponding lengths between image points ( $d_{12}, d_{13}, d_{23}$ ).  $D_{ij}$  denote the distances between vertices  $V_i$  and  $V_j$ . Similarly,  $d_{ij}$  denote the distances between vertices  $v_i$  and  $v_j$ . (For notation, please refer to Figure 4.)

$$s = \sqrt{\frac{b + \sqrt{b^2 - ac}}{a}} \tag{3}$$

$$(h_1, h_2) = \pm(\sqrt{(sD_{12})^2 - d_{12}^2}, \sigma\sqrt{(sD_{13})^2 - d_{13}^2}) \tag{4}$$

$$(H_1, H_2) = \frac{1}{s}(h_1, h_2) \tag{5}$$

Where:

$$a = (D_{12} + D_{13} + D_{23})(-D_{12} + D_{13} + D_{23})(D_{12} - D_{13} + D_{23})(D_{12} + D_{13} - D_{23}) \tag{6}$$

$$b = d_{12}^2(-D_{12}^2 + D_{13}^2 + D_{23}^2) + d_{13}^2(D_{12}^2 - D_{13}^2 + D_{23}^2) + d_{23}^2(D_{12}^2 + D_{13}^2 - D_{23}^2) \tag{7}$$

$$c = (d_{12} + d_{13} + d_{23})(-d_{12} + d_{13} + d_{23})(d_{12} - d_{13} + d_{23})(d_{12} + d_{13} - d_{23}) \tag{8}$$

$$\sigma = \begin{cases} 1 & \text{if } d_{12}^2 + d_{13}^2 + d_{23}^2 \leq s^2(D_{12}^2 + D_{13}^2 + D_{23}^2) \\ -1 & \text{otherwise} \end{cases} \tag{9}$$

$s$  – Scale;  $h_1, h_2, H_1, H_2$  – depths

The solution has two-way ambiguity except when  $h_1 = h_2 = 0$ . The ambiguity corresponds to a reflection about a plane parallel to image plane, since we cannot tell which of the points has smaller z-coordinate. To resolve this issue we proceeded by accounting for foreshortening of each triangle’s side separately. This was motivated by the observation that recovered three-point model varies under different scales in some range around previously estimated scale factor.

The detailed description of constraints to a solution are given in our previous work [12], as well as the procedure to calculate the rotation matrix  $R$  and translation vector  $t$ , which are used to define pose estimation. The proposed procedure estimates the relative pose, as there is no world coordinate frame with which to associate the head in the scene. We used image coordinate frame related to the image of frontal view ( $z=0$ ), but any other image coordinate frame is appropriate as well.

**Results:** The example of recovered 3D model points is given in Figure 5. Results are presented for yaw pose changes. The arrow showing the orientation in head images is a result of a back projection of a fourth vertex  $V_4$  to image plane. Since the pose recovery is affected by facial feature localization, our current efforts to improve the proposed method are oriented toward stabilization of feature detection and future work will be directed on verification of our results with our 3D measurement system XSense [21].

**Body orientation estimation based on inertial sensors and new two-layer stochastic filter architecture**

As already mentioned, inertial sensors have become attractive alternative to optoelectronic methods in the field of human motion tracking and detection. However, they rely on rather intensive signal processing algorithms in order to eliminate or reduce drawback of individual sensors (accelerometers, gyroscopes and magnetometers) like temperature drift, gravity bias and magnetic interference. This is in general achieved with some variant of Kalman filter or more recently particle filters.

Kalman filters are usually more computationally effective than particle filters (note computation times in Figure 6), but due to assumptions about linearity (depending on variant) and Gaussian distribution of process and measurement noises they might perform rather poor when compared to particle filters. This is depicted in Figure 6 where EKF stands for Extended Kalman filter. In order to overcome this we combined both estimators in two layer architecture with the aim of increasing computational efficiency while maintaining high level of accuracy [6]. Several different architectures were tested

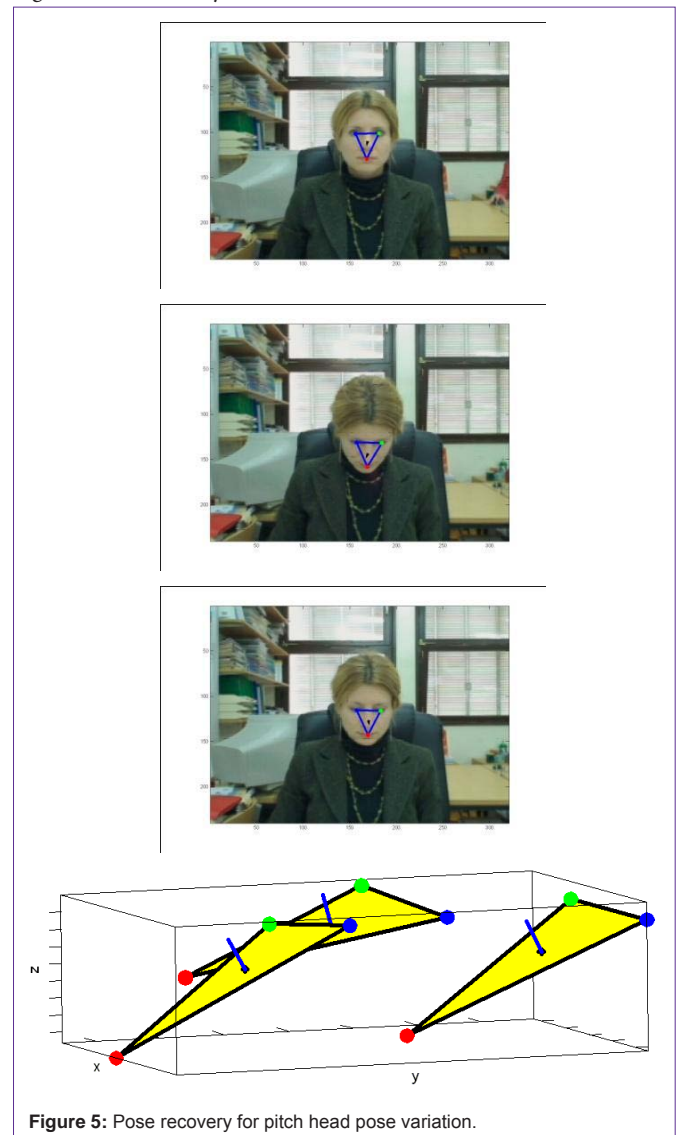


Figure 5: Pose recovery for pitch head pose variation.

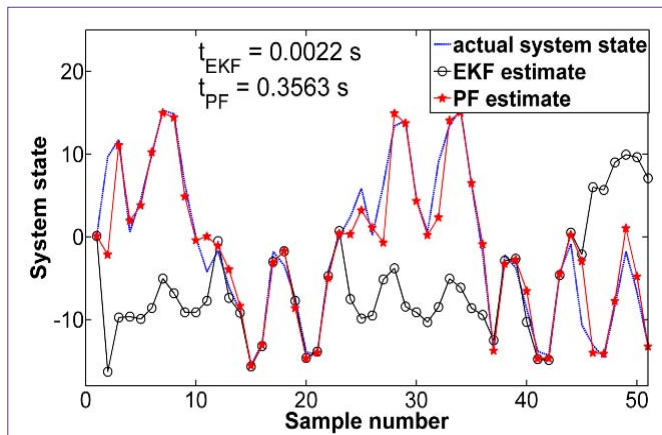


Figure 6: Example of Kalman filter poor performance in comparison to particle filter, in terms of accuracy.

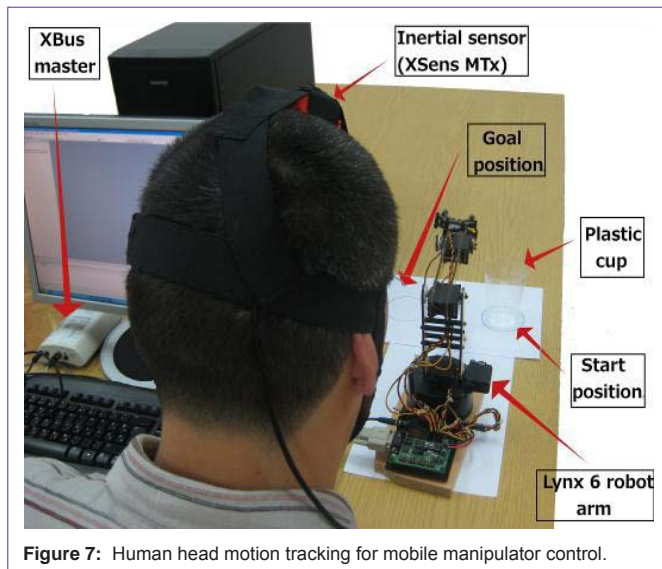


Figure 7: Human head motion tracking for mobile manipulator control.

on a problem of human head pose estimation with the aim of using head motion as a means of controlling computer pointer and different objects (like robot manipulator in Figure 7) by subjects with no control over upper limbs [22].

After testing several architectures both on simulated data and on real life data we found two layer scheme depicted in Figure 8 to perform best in terms of both accuracy and computational cost (indicated by required computational time). In this scheme layer 2 which contained particle filter was executed at highly reduced rate and was active when layer 1 was not active. Thus a good hand-off procedure was required. When going from layer 1 to layer 2 hand-off was achieved so that particle filter is presented to extended Kalman filter as additional measurement source with mean value and standard deviation calculated over all particles. Transition from layer 1 to layer 2 is made under assumption that gyroscopes biases cannot change significantly during those time instances when layer 2 is active thus they were not forwarded to that layer reducing computational time. Layer 1 output is then used to generate required number of particles based on Gaussian distribution with estimated value as mean and using calculated covariance matrix. Final output is current output from either layer 1 or layer 2 depending which time instance is

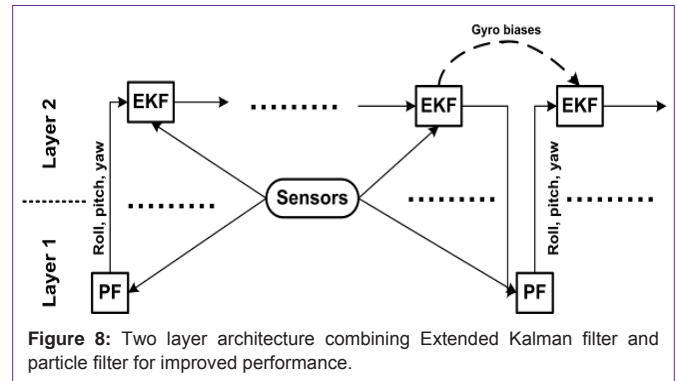


Figure 8: Two layer architecture combining Extended Kalman filter and particle filter for improved performance.

considered (i.e. which layer is currently active).

**Results:** Proposed scheme was tested on real life data recorded during mouse pointer control with human head. Obtained results (processed in batch mode) are presented in Table 2. Measurements from X Sense MTx sensors were used as baseline measurements. Procedure described above is annotated as Scheme 2 in the table. As can be seen from the table proposed scheme has the best combination of performance values: reasonably low computational time (about 4 times lower than standard particle filter) and good accuracy in terms of root mean square error (between 5-20% improvements in comparison to Extended Kalman filter).

To show practical applicability of the proposed architecture it was tested in real time scenarios of:

- 1.) text entry on virtual keyboard based on 15 test subjects with achieved performance of average typing speeds of 5.01 normalized words (5 characters including space) per minute
- 2.) Head gesture recognition with 15 test subjects based on discrete dynamic movement primitives as features. In total 6 different gestures were considered with average recognition rate of 77% using simple classificatory (based on correlation coefficient of calculated primitive weights).
- 3.) Control of robotic manipulator (Figure 7) using 3 test subjects on a task of relocating plastic cup from current to target location. Task was achieved successfully in all three instances with varying execution times and was aided with inclusion of an inverse robot model.

Thus we concluded that the proposed two layer architecture does indeed combine some of the positive qualities of Kalman and particle filters (as demonstrated in Table 2) and can be used in real time for practical applications. Possible future improvements

Table 2: Estimation results for real life human head pose .

Algorithm	Root mean square error [°]			Time [s]
	Roll	Pitch	Yaw	
EKF	1.49	1.42	2.63	0.37
PF	1.08	1.38	2.17	21.52
PF (simplified)	2.85	4.83	4.68	4.41
Scheme 1	1.14	1.24	3.5	4.92
Scheme 2	1.15	1.37	2.21	5.01
Scheme 3	0.92	1.68	2.72	155.66
Scheme 4	3.22	8.08	10.41	4.28

include implementation of adaptive extended Kalman filter, adaptive number of particle filter particles and inclusion of different hand-off procedures.

### Gesture recognition system based on MEMS accelerometer sensor

Another approach of implementation of inertial sensors is described in the following section. The rapid development of the MEMS sensor technology has inspired research in the field of accelerometer-based gesture recognition. This new, emerging interaction technique suits well the requirements in ubiquitous computing environments. Therefore, we focused our research toward the development of gesture recognition system based on 3D accelerometers embedded into smart phones.

Previous work on accelerometer-based gesture recognition mainly performed matching or modeling in time domain. The two main directions of presented research are Dynamic Time Warping (DTW)-based approach [23,24], and Hidden Markov Model (HMM)-based approach [25-27]. In our work, additional improvement is provided with introduction of adopted set of features used for recognition stage [15]. The developed system uses distance metric learning for Large Margin Nearest Neighbor (LMNN) classification in order to improve the results of classification and pattern recognition [14]. LMNN classification was proposed because it showed significant improvement on nearest neighbor classification using a Euclidean distance metric. After testing phase that was performed using MATLAB and PC computer, a prototype user application was developed on Google's Android platform to examine how the system performs in real life situations. Figure 9 presents the gesture recognition system architecture. In order to ease and to speed up interaction with a smart phone or some other mobile device, the device's built-in three-dimensional accelerometer is used. The system consists of a knowledge database that stores several sets of gestures and the corresponding execution actions, and a gesture recognizer algorithm that takes the tracking data obtained from the user and identifies the gestures. Whenever the user inputs a gesture, it is being picked up and recorded by the accelerometer sensor. The acceleration data is then filtered and feature extraction module codes it to a corresponding feature vector. In teaching mode, the gesture example feature vector is simply saved to the database with an appropriate label attached to it for future use, whilst in recognition mode, it is passed further to the classifier component that uses the preset several sets of gestures in the knowledge database to learn the distance metric and identify the most probable gesture. Finally, the result of the gesture recognition process launches the corresponding action.

The ongoing work is focused on extending the proposed system to include gesture spotting. In the current setup, the user needs to touch the screen of the device to indicate the beginning and the end of the gesture, which is not realistic. A more appropriate scenario would be to detect meaningful gesture traces from the stream of hand movements and recognizing them accordingly. Another interesting topic that is being explored is the issue of input device tilting, which can produce erroneous recognition results, if not taken into account. Additionally, we are planning to conduct a comprehensive, subjective user study that will help us evaluate the quality of user experience while running the system.

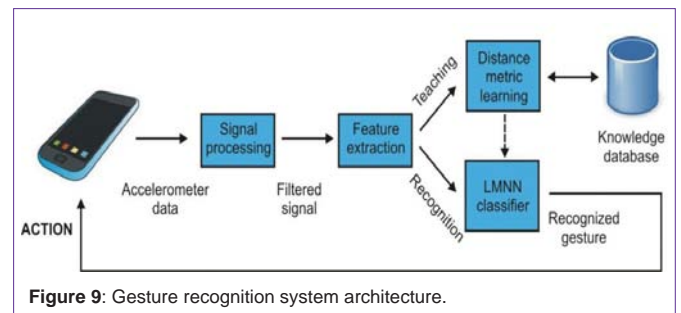


Figure 9: Gesture recognition system architecture.

## Biosignal Measurement, Analysis, Identification and Classification

### Processing and analysis of kinematics data measured during human gait

Our approach to the analysis of human (humanoid robot) gait was to propose the new kinematics parameters which would indicate the deviations of the gait of a particular subject from the normal gait pattern [7]. 3D gait kinematics was measured with the "in-house" made system, described in section 2.1. In order to provide a quantitative measure which would distinguish an irregular from a normal healthy gait pattern, we introduced five new kinematics parameters including the Gait Factor parameter (GF). Proposed Gait factor parameter is prominent to be the valuable measure for detection of irregularities in gait patterns of humans and humanoid robots.

**Measurement procedure:** The experiment included measurements on thirty healthy, barefoot humans while walking on a treadmill with normal natural gait and simulated irregular gait. Series of collection periods lasting no less than 1 min for each subject provided total of 150-200 gait cycles. In order to simulate irregular gait pattern, subjects were instructed to walk with artificial constrain on right knee. This procedure produced reduced mobility of a selected joint, thus causing irregular gait pattern. The kinematics of each joint were presented in a form of phase plots, closed 3D curves that portray the relationship between joint angle, angular velocity and acceleration, Figure 10. In order to compare an individual, potentially irregular gait trail with the normative (healthy gait), and to detect and evaluate the difference between irregular and normal gait pattern, we proposed a set of new kinematics parameters,  $E_n$ , for each analyzed joint ( $E_{n\_hip}$ ,  $E_{n\_knee}$ , and  $E_{n\_ankle}$ ). Each parameter is based on the calculation of Euclidian distance between points in phase plot of observed gait cycle and its corresponding normative phase plot. Second introduced parameter,  $PS_n$ , indicates the phase difference between the hip, knee, and ankle angle trajectories in phase plots for the normative and particular gait trial, Figure 10. The trajectory of phase shift plotted against the percentage of gait cycle shows us if gait events of particular subject are shifted according to the gait cycle of the normative gait. In order to establish a unique kinematics parameter which would indicate difference between normative gait trial and particular gait trial, we propose the third parameter, the gait factor,  $GF_n$ , which incorporates  $PS_n$  parameter and  $E_n$  for all joints contributing in the movement, and is defined as:

$$GF_n = \frac{1}{3} (E_{n\_hip} + E_{n\_knee} + E_{n\_ankle}) \cdot PS_n \quad (10)$$

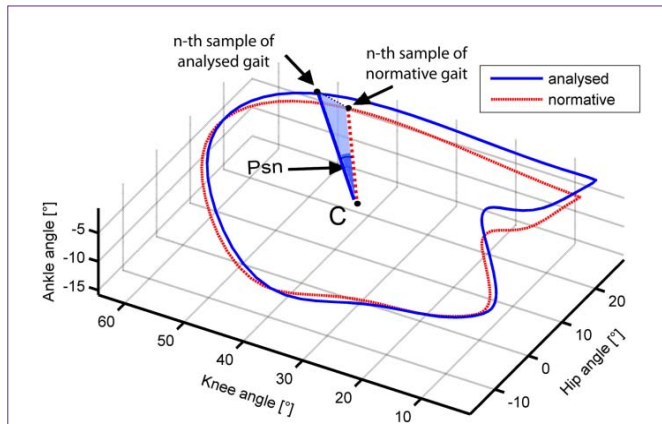


**Figure 10:** Hip angle - knee angle - ankle angle trajectories for normative gait cycle (dotted red line), and gait cycle measured on arbitrarily chosen subject (full blue line). Phase shift between two different gait cycles is denoted as Psn.

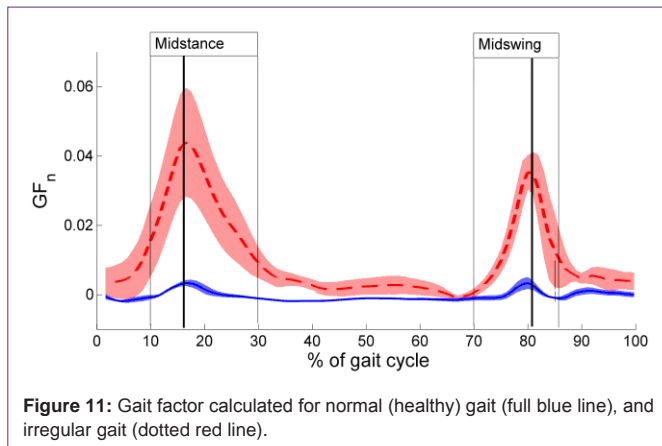


**Figure 11:** Gait factor calculated for normal (healthy) gait (full blue line), and irregular gait (dotted red line).

**Results:** We calculated the values of the proposed parameters for two types of gait: normal, healthy gait performed by healthy subject, and irregular gait simulated by wearing external knee constraints during walking trials. By focusing on the results shown in Figure 11, the difference between normal and irregular gait patterns is clearly indicated. Moreover, exact moment or phase in gait cycle could be determined where large irregularities are observed. As a future work idea, application of the proposed method on other cyclic movements like pedaling or rowing is also an option.

**Automatic classification of infant sleep based on instantaneous frequencies in a single-channel EEG signal**

There have been numerous studies related with sleep stage classification, which have confirmed that feature extraction plays an important role for success of the proposed methods. In addition, more than 70 different features have been tested for sleep stage classification [28]. Our approach toward biosignal research was to develop the automatic sleep stage classification based on features of only the Electroencephalogram (EEG) signals [8]. EEG signals (Figure 12) are in constant research focus of numerous biomedical engineering researchers. Our aim was to find a feature inside EEG signal that represents the time sequence of a signal according to the physical meaning of the sleep stage we wanted to identify the signal with. Our hypothesis was that features that better describe sleep stage

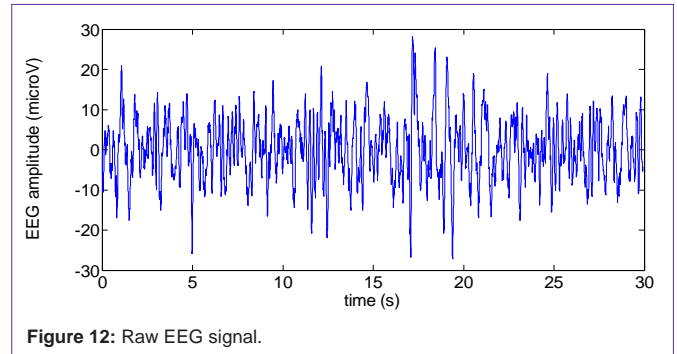


**Figure 12:** Raw EEG signal.

specificities could be extracted from a signal if it was decomposed into components that reflected the true physical processing. Thus, the kernel is not known in advance and the nature of the signal is acquired by applying the appropriate decomposition mode.

**Methods:** As a time-frequency method, designated for nonlinear and non-stationary signals, the Empirical Mode Decomposition method (EMD) was selected for the basic decomposition procedure because it embeds the basic idea of the proposed hypothesis [29]. It decomposes the signal into Intrinsic Mode Functions (IMF) with corresponding frequency ranges that characterize well the appropriate oscillatory modes embedded in the brain neural activity acquired by EEG [30].

The new approach presented in this study includes the introduction of new features derived from IMFs. To calculate the instantaneous frequency of IMFs, an algorithm was developed using the Generalized Zero Crossing method. With the resulting frequencies, we can demonstrate that during one 30 s epoch, the EEG signal changes its instantaneous frequency more often if it belonged to an active sleep stage than if it belonged to a quiet sleep stage epoch. Considering this frequency dynamic, we proposed the new feature, which describes how many times the instantaneous frequency changes during one 30 s epoch (IMF frequency change). An additional new feature affecting the classification of sleep stages was the median value of instantaneous frequency (IMF med frequency), which exhibited higher values in REM than in NREM sleep stages in the first seven IMFs contained in the EEG signals. The Relative Power Spectral Density (RSD) of the EEG signal at characteristic frequency bands was selected as the reference point feature to validate the efficiency of the sleep stage classification of our proposed features. To achieve a more accurate automatic classification, a hybrid feature was created by combining two different types of EEG features, the spectral feature and time-frequency feature.

**Results:** The sleep stage classification, based on the novel feature vectors of a single EEG channel, for the daytime sleep of 20 healthy Croatian babies aged three months, was performed using the SVM classification algorithm. The results were evaluated by applying the cross-validation method to achieve approximately 90% accuracy (Figure 13) and with new examinee data achieving 80% average accuracy classification (Figure 14). The obtained results were higher than the results for classification using only the RSD feature, and higher than the human experts' agreement [31,32], which positioned the method, based on the proposed features, as an efficient procedure for automatic sleep stage classification. In our future work we plan to

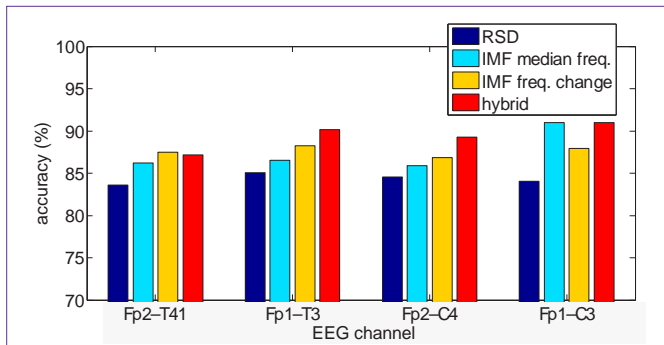


Figure 13: Accuracy of the automatic sleep stage classification from 10-fold cross validation procedure.

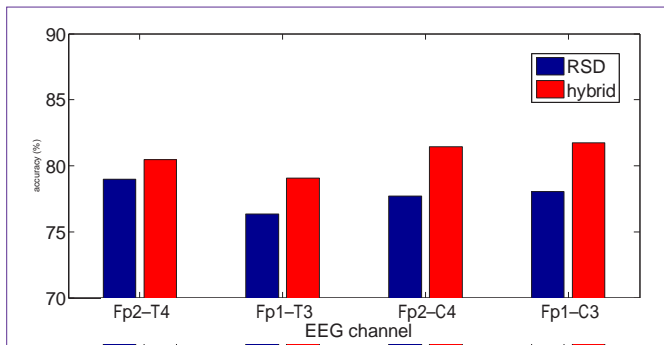


Figure 14: Accuracy of the automatic sleep stage classification of the new examinee signal.

study the potential of the newly proposed EEG features to highlight the congruence of twin pairs, indicating the genetic determination of sleep.

### Improved Structured Light 3D Scanner for Anthropometric Parameter Estimation

Cost effective estimation of anthropometric parameters used in biomechanical analysis is still open research issue due to the desire for increased accuracy with off-the-shelf components. This is in turn motivated by the observations that inverse dynamic’s results can differ significantly depending on accuracy of used anthropometric parameter [4]. Thus we wanted to improve on available 3D structured light scanners while keeping costs at acceptable level. Additionally we wanted our new structured light pattern to be robust to small subject movements and possible light reflections, which led to introduction of scanning stripes at the end of patter cycle. This was achieved with kind of stereovision system with one active sensor (LPD projector) and one passive sensor (camera) [5]. In order to evaluate newly proposed scanning pattern we carried out experimental measurements with 8 test subjects. Example of measurement setup can be seen in Figure 15. Measurements were achieved with new light structure pattern as well as standard one (for comparison reasons) while immersion method was used as baseline measurement method. In addition testing was done on artificial objects (measurement etalons, boxes, tubes and life size mannequin) with known geometrical properties and under significantly different conditions (e.g. vibration induced by vibrating motors to simulate small subject movements; different surface textures to simulate different cloths subjects might wear etc.).

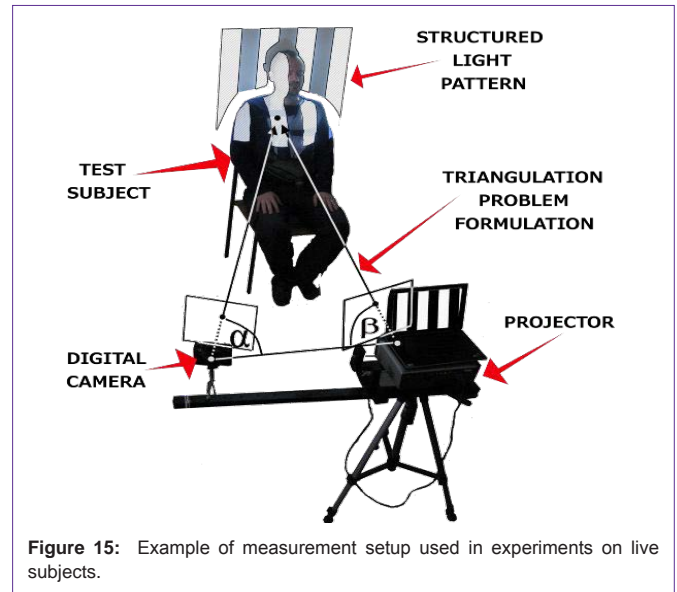


Figure 15: Example of measurement setup used in experiments on live subjects.

### Results

Obtained results for static objects are depicted in Figure 16, which in terms of used calibration object size were 0.38% for *x* axis, 0.12% for *y* axis and 1.7% for *z* axis. Associated root mean square errors were: 4.24mm, 2.34mm and 1.62mm for corresponding axis. This demonstrated that scanner performed well for simple 3D objects. The mean error was around 0 (0.14 ml) with highest being for subject 4 with 1.89 ml. This led to total error estimation of a whole segment under 1% with rather high standard deviation of about 10%. Such high deviance was attributed to imperfections of immersion method and setup as well as relatively small measurement increments used (1cm). Results from the mannequin had similar mean values but significantly lower deviations (about 50% less) which indicated that subject movements during immersion measurements might have also contributed to larger standard deviation values. Finally, to illustrate system accuracy, segment-by-segment comparison between three methods used in the study for forearm volume estimation (and subsequently mass estimation) is presented in Figure 17. From figure it can be concluded that newly proposed structured light pattern follows better immersion curve than standard light structure with RMSE value of 3.42 ml compared to 4.59 ml (which is improvement of about 25%). For mass estimation we compared our method and

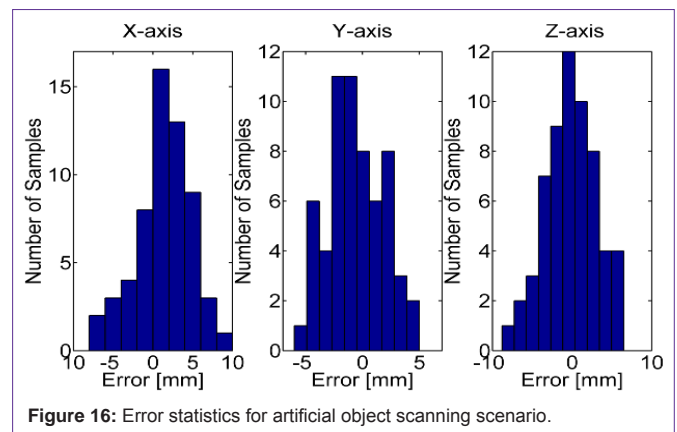
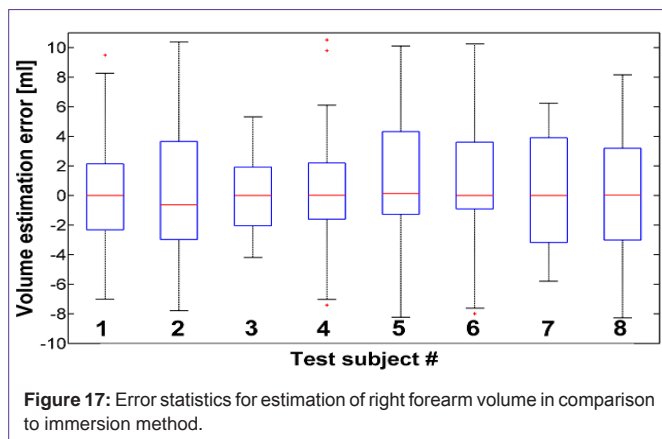


Figure 16: Error statistics for artificial object scanning scenario.

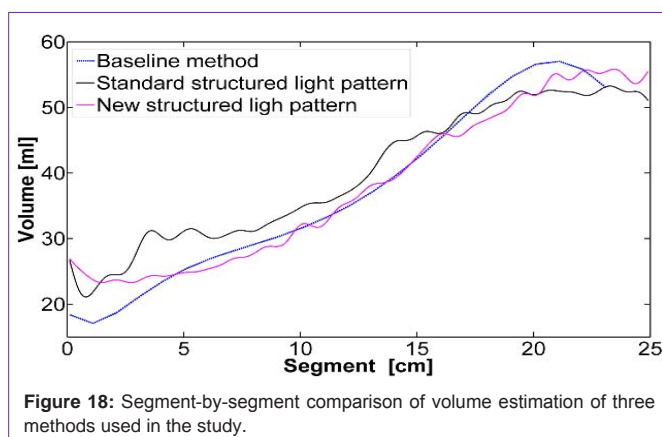


standard structured light method to de Leva anthropometric tables which are widely used in biomechanics research. Here improvement was also present but with smaller value of about 17%.

Next, results for all eight subjects (forearm volume estimation) are presented in Figure 18. In comparison to baseline measurements. Tests performed on live subjects and artificial objects in different conditions demonstrated viability of our new approach. However, there is still room for improvement such as inclusion of sub-pixel accuracy, simultaneous scanning with two units to fully capture segment of interest in one swipe and combining these results with mass distribution information or human segment density profiles.

## Conclusion

Biomedical engineering is a highly interdisciplinary and well established discipline spanning across engineering, medicine and biology. Rapid technological developments in the last century have brought the field of biomedical engineering into a totally new realm [33]. The expansion of biomedical engineering research is markedly obvious in the past ten years. As a result, the field of biomedical engineering is thriving, with innovations that aim to improve the quality of human life and reduce the cost of medical care [33]. This paper presents some of recent trends in biomedical engineering, with a particular focus on the field of biomechanics (human motion tracking based on 3D optical motion capturing systems, and motion detection based on inertial sensors, computer vision and image processing), biosignal measurement, processing, analysis and classification, and human anthropometric parameters estimation. Each section includes



ideas and guidelines for future work, as well. This wide range of topics provide a valuable update to researchers in the multidisciplinary area of biomedical engineering and an interesting introduction for engineers new to the area.

## References

1. Knudson D. *Fundamentals of Biomechanics*. New York: Kluwer Academic/Plenum Publishers. 2003.
2. Devasahayam SR. *Signals and Systems in Biomedical Engineering*. New York: Kluwer Academic/Plenum Publishers. 2000.
3. Stancic I, Grujic T, Panjkota A. Design, development, and evaluation of optical motion-tracking system based on active white light markers. *IET Science, Measurement & Technology*. 2013; 7: 206-214.
4. Music J, Kamnik R, Munih M. Model based inertial sensing of human body motion kinematics in sit-to-stand movement. *Simulation Modelling Practice and Theory*. 2008; 16: 933-944.
5. Stancic I, Music J, Zanchi V. Improved structured light 3D scanner with application to anthropometric parameter estimation. *Measurement*. 2013; 46: 716-726.
6. Music J, Cecic M, Zanchi V. Real-time body orientation estimation based on two-layer stochastic filter architecture. *Automatika: Journal for Control, Measurements, Electronics, Computing and Communications*. 2010; 51: 264-274.
7. Stancic I, Grujic T, Bonkovic M. New kinematic parameters for quantifying irregularities in the human and humanoid robot gait. *International Journal of Advanced Robotic Systems*. 2012; 9: 215.1-215.8
8. Cic M, Soda J, Bonkovic M. Automatic classification of infant sleep based on instantaneous frequencies in a single-channel EEG signal. *Computers in biology and medicine*. 2013; 43: 2110-2117.
9. Windolf M, Götzen N, Morlock, M. Systematic accuracy and precision analysis of video motion capturing systems-exemplified on the vicon-460 system. *Journal of Biomechanics*. 2008; 41: 2776-2780.
10. Maletsky LP, Sun J, Morton NA. Accuracy of an optical active-marker system to track the relative motion of rigid bodies. *Journal of Biomechanics*. 2007; 40: 682-685.
11. Plestina V, Papić V. Object classification in water sports. *Proceedings of the 18th IEEE symposium on Computers and Communications – ISCC*. Split, Croatia. 2013.
12. Kuzmanic Skelin A, Bonkovic M, Papić V. Measurement of head rotation using triangular face model. *Proceedings of 7th IASTED International Conference on Biomedical Engineering*; Innsbruck, Austria. 2010.
13. Music J, Murray-Smith R. Virtual hooping: teaching a phone about hula-hooping for fitness, fun and rehabilitation. *Proceedings of MobileCHI*. Lisbon, Portugal. 2010.
14. Marasovic T, Papić V. Accelerometer based gesture recognition system using distance metric learning for nearest neighbor classification. *Proceedings of IEEE International Workshop on Machine Learning for Signal Processing (MLSP)*. 2012.
15. Marasovic T, Papić V. A novel feature descriptor for gesture classification using smartphone accelerometers. *Proceedings of the 18th IEEE symposium on Computers and Communications – ISCC*. 2013.
16. Iwase S, Saito H. Parallel tracking of all soccer players by integrating detected positions in multiple view images. *Proceedings of the IEEE International Conference on Pattern Recognition of the IEEE Computer Society*. 2004.
17. Pers M, Kristan M, Pers J, Kovacic S. A template-based multi-player action recognition of the basketball game. *Proceedings of the ECCV Workshop on Computer Vision Based Analysis in Sport Environments*. 2006.
18. Taylor CJ. Reconstruction of articulated objects from point correspondence using a single uncalibrated image. *Computer Vision and Image Understanding*. 2000; 80: 349-363.

19. Farkas L. Anthropometry of the Head and Face. New York: Raven Press. 1994.
20. Alter TD. 3-D pose from 3 points using weak perspective. IEEE Trans. on Pattern Analysis and Machine Intelligence. 1994; 16: 802-808.
21. Xsens – the leading innovator in 3D motion tracking technology.
22. Music J, Cecic M, Bonkovic M. Testing inertial sensor performance as hands-free human-computer interface. WSEAS Transactions on Computers. 2009; 8: 715-724.
23. Niezen G, Hancke GP. Gesture recognition as ubiquitous input for mobile phones. Proceedings of DAP (Devices that Alter Perception) Workshop at the 10<sup>th</sup> International Conference on Ubiquitous Computing (UBICOMP'08). 2008.
24. Liu J, Zhong L, Wickramasuriya J, Vasudevan V. Accelerometer - based personalized gesture recognition and its applications. Pervasive and Mobile Computing. 2009; 5: 657–675.
25. Schlomer T, Poppinga B, Henze N, Boll S. Gesture recognition with a Wii controller. Proceedings of 2nd International Conference on Tangible and Embedded Interaction. 2008; 11-14.
26. Mantyla VM. Discrete hidden Markov models with application to isolated user-dependent hand gesture recognition. VTT Publications. 2001.
27. Kela J, Korpipaa P, Mantyjärvi J, Kallio S, Savino G, Jozzo L, et al. Accelerometer based gesture control for a design environment. Personal Ubiquitous Computing. 2006; 10: 285–299.
28. Susmakova K, Krakovska A. Discrimination ability of individual measures used in sleep stages classification. Artif Intell Med. 2008; 44: 261-277.
29. Li X. Temporal structure of neuronal population oscillations with empirical model decomposition. Phys. Letters A. 2006; 356: 237–241.
30. Junsheng C, Dejie Y, Yu Y. Research on the intrinsic mode function (IMF) criterion in EMD method. Mech. Syst. Signal Processing. 2006; 20: 817–824.
31. Charbonnier S, Zoubek L, Lesecq S, Chapotot F. Self-evaluated automatic classifier as a decision-support tool for sleep/wake staging. Comput Biol Med. 2011; 41: 380-389.
32. Anderer P, Gruber G, Parapatics S, Woertzc M, Miazhynskaia T, Klösch G, et al. An E-health solution for automatic sleep classification according to rechtschaffen and kales: validation study of the somnolyzer 24x7 utilizing the siesta database. Neuropsychobiology. 2005; 51: 115–133.
33. Laskovski AN. Biomedical Engineering: Trends in Materials Science. Rijeka: Intech Press. 2011.